

Otic Mesenchyme Cells Regulate Spiral Ganglion Axon Fasciculation through a Pou3f4/EphA4 Signaling Pathway

Thomas M. Coate,^{1,*} Steven Raft,² Xiumei Zhao,³ Aimee K. Ryan,⁴ E. Bryan Crenshaw III,⁵ and Matthew W. Kelley¹

¹Laboratory of Cochlear Development

²Sensory Cell Regeneration and Development Section

National Institute on Deafness and Other Communication Disorders, National Institutes of Health, Bethesda, MD 20892, USA

³Department of Biology, Georgetown University, Washington, D.C. 20057, USA

⁴Department of Pediatrics, McGill University, Research Institute of the McGill University Health Centre, Montreal, Quebec H3A 2T5, Canada

⁵Children's Hospital of Philadelphia, University of Pennsylvania, Philadelphia, PA 19104, USA

*Correspondence: coatet@nidcd.nih.gov

DOI 10.1016/j.neuron.2011.10.029

SUMMARY

Peripheral axons from auditory spiral ganglion neurons (SGNs) form an elaborate series of radially and spirally oriented projections that interpret complex aspects of the auditory environment. However, the developmental processes that shape these axon tracts are largely unknown. Radial bundles are comprised of dense SGN fascicles that project through otic mesenchyme to form synapses within the cochlea. Here, we show that radial bundle fasciculation and synapse formation are disrupted when *Pou3f4* (DFNX2) is deleted from otic mesenchyme. Further, we demonstrate that *Pou3f4* binds to and directly regulates expression of *Epha4*, *Epha4*^{-/-} mice present similar SGN defects, and exogenous *EphA4* promotes SGN fasciculation in the absence of *Pou3f4*. Finally, *Efnb2* deletion in SGNs leads to similar fasciculation defects, suggesting that ephrin-B2/EphA4 interactions are critical during this process. These results indicate a model whereby *Pou3f4* in the otic mesenchyme establishes an Eph/ephrin-mediated fasciculation signal that promotes inner radial bundle formation.

INTRODUCTION

Hearing depends on hair-cell-mediated conversion of sound stimuli into electrochemical information that is then relayed to the brain via spiral ganglion neurons (SGNs), a cluster of bipolar afferent neurons that parallel the medial surface of the cochlear coil. Although considerable research has been conducted on the patterning of the hair cells and support cells within the cochlea (Driver and Kelley, 2009; Kelley, 2006; Puligilla and Kelley, 2009), relatively little work has focused on mechanisms that control the patterning, migration, and outgrowth of the SGNs (reviewed in Appler and Goodrich, 2011). As essential regulators of

auditory information, a better understanding of how these processes occur within SGNs will enhance our understanding of auditory function, as well as how neural connections might be reformed in cases of deafness.

During development, immature proliferating neuroblasts delaminate from the otocyst (Ruben, 1967) and migrate to form a dense ganglion along the medial side of the inner ear epithelium. As development continues, developing SGNs extend peripheral axons through the surrounding (otic) mesenchyme cells (Carney and Silver, 1983) and subsequently penetrate the cochlear epithelium to form glutamate-responsive ribbon-type synapses with inner and outer hair cells (Smith, 1961). During this process, SGN axons form a series of dense fascicles, referred to as inner radial bundles, each of which contains fibers with similar frequency tuning. Groundbreaking work has begun to delineate the regulatory networks that establish the circuitry between the cochlea and the central nervous system (CNS) (Koundakjian et al., 2007); however, specific mechanisms regulating SGN developmental patterning are unknown.

The POU-domain (Pit1-Oct1/2-unc86) proteins are a phylogenetically conserved family of transcription factors with diverse DNA-binding affinities and a wide range of developmental functions (Phillips and Luisi, 2000; Ryan and Rosenfeld, 1997). Mutations in *POU3F4/Pou3f4*, located on the X chromosome, cause deafness in humans (DFNX2) and mice (Kandpal et al., 1996; Minowa et al., 1999). Expression studies indicate that *Pou3f4* expression is restricted to otic mesenchyme cells, with limited or no expression in the hair cells or SGNs (Minowa et al., 1999; Phippard et al., 1998; Samadi et al., 2005). Consistent with this, the cochlear sensory epithelium (organ of Corti), which includes hair cells and supporting cells, appears normal in *Pou3f4*^{-/-} mice. However, the cochlear duct has been described as dysplastic with a moderate length reduction, possibly owing to disorganization and altered morphology of otic mesenchyme cells (Minowa et al., 1999; Phippard et al., 1999). Considering the intimate relationship between developing SGNs and otic mesenchyme, defects in aspects of SGN formation in the absence of *Pou3f4* seemed possible.

Any effects of *Pou3f4* on SGN formation would most likely be indirect and therefore mediated by other factors. In particular,

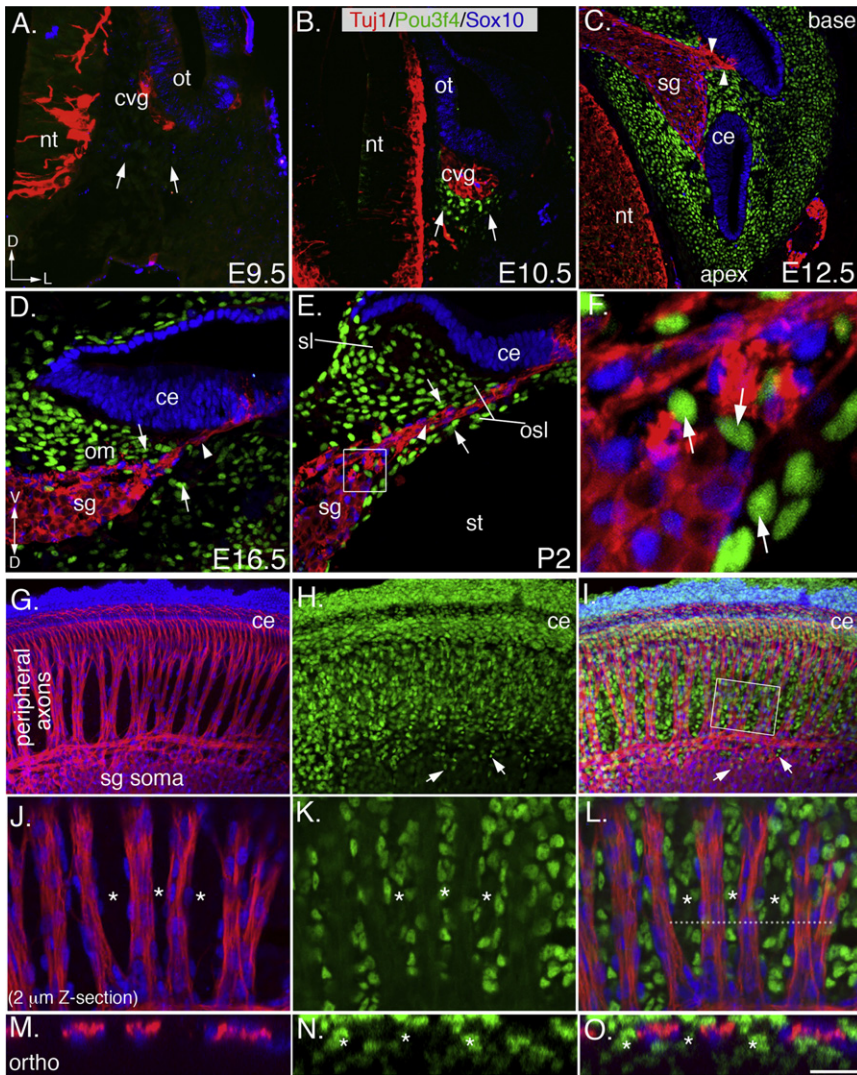


Figure 1. Pou3f4 Expression during SGN Development in Mouse

(A) At E9.5, there is no Pou3f4 expression in the presumptive otic mesenchyme (arrows). nt, neural tube; ot, otocyst; cvg, cochleovestibular ganglion; D, dorsal; L, lateral.

(B) At E10.5, Pou3f4 expression commences in the otic mesenchyme (arrows).

(C) At E12.5, SGN peripheral axon outgrowth has started (arrowheads), and Pou3f4 protein is expressed by all mesenchyme cells in the otic capsule. sg, spiral ganglion; ce, cochlear epithelium.

(D) Midmodiolar cross-section at E16.5. SGNs' peripheral axons (arrowhead) project through otic mesenchyme (arrows) to reach the cochlear epithelium. om, otic mesenchyme; V, ventral.

(E) At P2, SGNs and glia (arrowhead) are clearly separated from the surrounding mesenchyme (arrows). st, scutum tympani; osl, osseous spiral lamina; sl, spiral limbus.

(F) High-magnification image from the boxed region in (E). Pou3f4-positive cells (arrows) within the ganglion do not express neuron or glia markers.

(G–I) Whole-mount view of the spiral ganglion and otic mesenchyme at E17.5. Inner radial bundles extend through otic mesenchyme to the cochlear epithelium. Arrows in (H) and (I) point to mesenchyme cells analogous to those illustrated in (F).

(J–L) A 2-μm-thick confocal z stack from the boxed region in (I) illustrates the separation of the axons of the radial bundles and the mesenchyme cells. Asterisks mark bands of mesenchyme.

(M–O) An orthogonal projection derived from the region indicated by the dotted line in L. The asterisks delineate the bands of mesenchyme. For (A)–(C) and (G)–(I), the length of the scale bar in (O) represents 150 μm; for (D) and (E), the length of the scale bar in (O) represents 50 μm; for (F), the scale bar in (O) represents 10 μm; for (J)–(L), the length of the scale bar in (O) represents 30 μm; for (M)–(O), the length of the scale bar in (O) represents 20 μm.

Eph receptors, the largest family of vertebrate receptor tyrosine kinases, are known to interact with ephrin ligands to generate both forward and reverse signals and have been linked extensively with axon guidance (Coate et al., 2009; Huai and Drescher, 2001; Pasquale, 2005; Wilkinson, 2001). Although several studies have documented the presence of Ephs and ephrins in the inner ear (Bianchi and Gale, 1998; Zhou et al., 2011), a role for fasciculation and/or radial bundle formation has not been described.

RESULTS

Pou3f4 Is Expressed by Otic Mesenchyme Cells during All Stages of SGN Development

Pou3f4 expression in the otic mesenchyme has been described previously (Ahn et al., 2009; Phippard et al., 1998), but those studies did not determine whether other cells nearby, such as SGNs or associated glia, were also positive for Pou3f4. Thus, we conducted a comprehensive temporal and spatial analysis of

Pou3f4 protein expression during SGN development using a Pou3f4-specific antibody, along with markers of mature auditory neurons (Tuj1) and Schwann cells (Sox10; Puligilla et al., 2010). In mice, SGNs develop within the cochleovestibular ganglion (cvg), a transient structure formed by neuroblasts that delaminate from the ventral-medial side of the otocyst at embryonic day (E) 9.5 (Figures 1A and 1B). At E9.5, Pou3f4 expression in the presumptive mesenchyme is not detectable (Figure 1A); however, at E10.5, small patches of Pou3f4-expressing mesenchyme cells emerge adjacent to the cvg (Figure 1B, see arrows). By E12.5, when the auditory and vestibular components of the inner ear have diverged (Koundakjian et al., 2007), Pou3f4 is detectable in all compartments of the otic mesenchyme (Figure 1C). At this stage, neural crest-derived Schwann cells infiltrate the ganglia, and SGNs begin to project peripheral axons toward the prosensory domain located within the cochlear epithelium (Carney and Silver, 1983). At these early stages, Pou3f4 is detectable in otic mesenchyme cells, but not in neurons, glia, or epithelia. Moreover,

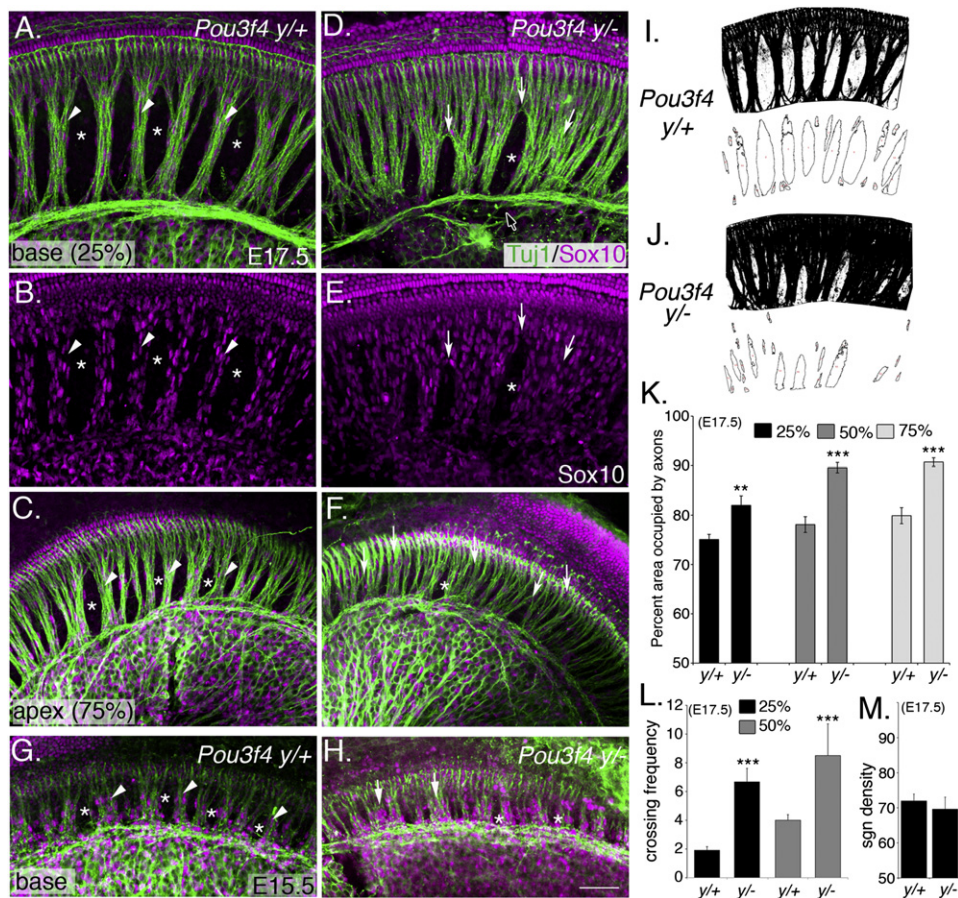


Figure 2. Absence of *Pou3f4* Causes Defects in Fasciculation of Inner Radial Bundles

(A–C) Representative images of the base (A) and apex (C) from a *Pou3f4*^{+/+} cochlea at E17.5. Arrowheads point to appropriately formed inner radial bundles; asterisks label bands of otic mesenchyme cells.

(D–F) Whole-mount images as in (A)–(C) but from *Pou3f4*^{-/-}. Arrows point to defasciculated axons. The black arrow (with white stroke) points to the intraganglionic spiral axon bundle (Simmons et al., 2011) that also shows fasciculation defects.

(E) Glial cells display a similar ectopic pattern.

(G) At E15.5, the inner radial bundles are apparent (arrowheads), as well as regions of mesenchyme (asterisks).

(H) *Pou3f4*^{-/-} cochlea at E15.5. Fasciculation defects are already evident. Scale bar represents 50 μm.

(I and J) Illustration of the scheme by which the radial bundle phenotype was quantified.

(K and L) Histograms illustrating significant increases in axon fasciculation defects (K) and the number of times per 500 μm that individual processes cross between fascicles (L) in *Pou3f4*^{-/-} cochleae. Percentages indicate the position along the length of the cochlea with respect to the distance from the base. **p ≤ 0.01; ***p ≤ 0.001.

(M) The density of neurons along the length of the cochlea is unchanged between *Pou3f4*^{+/+} and *Pou3f4*^{-/-} mice.

(K–M) Mean ± SEM. Scale bar represents 50 μm.

Pou3f4-expressing mesenchyme cells appear to make direct contact with the distal ends of the SGN peripheral axons (Figure 1C, arrowheads) in regions where Schwann cells have not yet arrived. At E16.5, SGN peripheral axon outgrowth continues along the length of the cochlea as the otic mesenchyme (om) population expands to form the future osseous spiral lamina and spiral limbus (osl and sl, respectively; Figures 1D and 1E). The adult osl consists of bony plates that surround the SGN axons, and the sl is a thickened periosteum. At E15.5–E16.5, radial bundles form concurrently with the appearance of bands of mesenchyme cells located between SGN peripheral axons (as in Figure 2G, asterisks). By P2, *Pou3f4*-positive mesenchyme cells segregate from

extending SGN axons, with clearly visible boundaries (Figure 1E). Occasional *Pou3f4*-positive cells were observed within the somal layer of the spiral ganglion (Figure 1E), but these cells were not positive for either Tuj1 or Sox10, suggesting that they are mesenchyme cells that have interspersed the ganglion during development (arrows in Figures 1E and 1F). In whole mount at E17.5, the segregation of the peripheral axons and the otic mesenchyme is dramatic: groups of ~50–100 axons fasciculate to form relatively evenly spaced inner radial bundles along the length of the cochlea (Figures 1G–I). Higher-magnification images show how axons travel in areas that are devoid of *Pou3f4* and rarely cross between bundles (Figures 1J–O).

Radial Bundle Fasciculation Is Lost in *Pou3f4^{y/+}* Embryos

Previously, *Pou3f4* mutants were shown to have variable levels of hypoplasia of the otic mesenchyme and severe hearing impairment (Minowa et al., 1999; Phippard et al., 1999). Therefore, we hypothesized that if SGN fasciculation and otic mesenchyme organization are interdependent, then inner radial bundle formation may require *Pou3f4*. To test this hypothesis, we compared radial bundle development in whole-mount preparations of *Pou3f4^{y/+}* and *Pou3f4^{y/-}* cochleae (Figures 2A–2H). At E17.5, *Pou3f4^{y/+}* cochleae contained dense, well-organized fascicles that projected directly from the SGN soma to the cochlear epithelium (Figures 2A–2C). This pattern is most conspicuous at the base of the cochlea (Figures 2A and 2B) but is also evident at the apex (Figure 2C), where the bundles are always less compact. In contrast, SGN axons in *Pou3f4^{y/-}* embryos failed to fasciculate properly, formed loosely compacted bundles, and contained increased numbers of laterally projecting processes (Figures 2D–2F). Although this fasciculation phenotype could arise from a deficit of auditory glia (Breuskin et al., 2010), there appeared to be no defect in their development (Figure 2E; Sox10 staining). Fasciculation defects were evident in *Pou3f4^{y/-}* embryos as early as E15.5 (Figures 2G and 2H), suggesting disruptions during the early phases of axon outgrowth.

To quantify fasciculation along the length of the cochlea, we measured the total area occupied by SGN axons between the soma and the sensory epithelium (see Experimental Procedures; Figures 2I and 2J). In base, middle, and apical regions of the cochlea, the SGN axons in *Pou3f4^{y/-}* embryos consumed significantly more space compared to their wild-type littermates (Figure 2K), with the greatest difference in fasciculation present at the apex (80% versus 91%, respectively; see Figure 2K, light gray bars). In addition, the frequency with which processes crossed between fascicles was significantly greater in *Pou3f4^{y/-}* embryos compared to wild-type (Figure 2L; arrows in Figure 2D). *Pou3f4^{y/-}* cochleae have been reported to be slightly shorter than controls, which raised the possibility that the SGN fasciculation defects might result from changes in neuron numbers along the length of the cochlea. However, a comparison of the density of SGN cell bodies between *Pou3f4^{y/+}* and *Pou3f4^{y/-}* cochleae indicated no significant differences (Figure 2M; see also Figure S1 available online).

To determine whether a loss of surrounding otic mesenchyme cells caused the SGN fasciculation defects in *Pou3f4^{y/-}* mice, we compared the frequency of apoptotic cells in the otic mesenchyme between *Pou3f4^{y/+}* and *Pou3f4^{y/-}* animals using antibodies against cleaved caspase-3 (CC3) (Figures S1E–S1J). We also used DAPI to look for potential necrotic lesions (Figures S1L–S1O). Although the density of the mesenchyme cells appeared to be slightly lower in *Pou3f4^{y/-}* animals (compare the outlined areas in Figures S1G and S1J), there was no enhanced apoptosis or necrosis in the otic mesenchyme cells (Figures S1K–S1O).

Innervation and Ribbon Synapse Formation Are Diminished in *Pou3f4^{y/-}* Embryos

Axon fasciculation reduces pathfinding errors and provides efficient innervation of target tissues (Tessier-Lavigne and Goodman, 1996). Considering the fasciculation defects in the *Pou3f4^{y/-}* cochleae, we examined possible changes in innerva-

tion. SGNs are subdivided into two classes: type I SGNs (90% of the entire population), which form synapses on inner hair cells, and type II SGNs (the remaining 10%), which grow past the inner hair cell layer, cross the tunnel of Corti, and then turn toward the base before forming synapses with outer hair cells (Huang et al., 2007; Koundakjian et al., 2007). At the base of wild-type cochleae at E17.5, Tuj-1 immunolabeling shows the dense layer of type I SGN endings, as well as type II processes that cross the pillar cell layer before turning toward the base (Figure 3A). These preparations were counterstained with Sox10 antibodies to reveal the morphology of the cochlear epithelium with respect to the SGNs (Figures 3B and 3C). Images acquired at the mid-base, midapex, and apex (Figures 2D–2F) illustrate the base-to-apex maturation of the type II processes. In comparison with *Pou3f4^{y/+}* embryos, *Pou3f4^{y/-}* embryos at E17.5 showed diminished innervation by both types of SGNs: the type I layer of *Pou3f4^{y/-}* embryos was narrowed and less robust (see brackets, Figures 3G–3L), and the number of type II processes was substantially reduced (Figures 3G–3L). In addition, the type II processes that were present appeared to be shorter and less mature (Figures 3J and 3K) or had not extended (Figure 3L). Sox10 immunostaining indicated no changes in the morphology of the supporting cells in *Pou3f4^{y/-}* cochleae (Figures 3H and 3I). These data suggest that fasciculation defects result in diminished target innervation within the cochlear epithelium.

We therefore reasoned that synapse numbers between SGNs and hair cells would also be reduced in *Pou3f4^{y/-}* mice. In hair cells, ~500 nm ribbon-type synapses can be visualized and quantified using anti-Ribeye antibodies (Meyer et al., 2009; Figures 3M–3P). Postsynaptic glutamate receptor immunoreactivity has a diffuse appearance at early postnatal stages but is suitable for qualitative observations (Nemzou N et al., 2006; Figures 3M–3P). Comparisons at postnatal day eight (P8) indicated fewer ribbon synapses and lower levels of glutamate receptor immunoreactivity in *Pou3f4^{y/-}* mice (Figures 3M–3P). Cross-sections of cochleae at P8, immunostained with neurofilament and Ribeye antibodies, confirmed a decrease in the density of type I SGN endings and showed a quantifiable decrease in the number of ribbon synapses (Figures 3Q–3X). Consistent with the gradient in innervation defects, the decrease in ribbon synapses was also graded with a mild effect in the base of the cochlea and a more severe effect at the apex (reduced by approximately 30%). These data suggest that disrupting fasciculation impairs the ability of SGNs to locate their targets and form synapses.

Expression of EphA4 Is Reduced in Otic Mesenchyme Lacking Pou3f4

Fasciculation is typically mediated by cell-surface or secreted factors (Tessier-Lavigne and Goodman, 1996); therefore, we hypothesized that otic mesenchyme cells from *Pou3f4^{y/-}* mice might fail to express one or multiple factors that directly promote SGN fasciculation. Microarray results (see Experimental Procedures) comparing mRNAs from *Pou3f4^{y/+}* and *Pou3f4^{y/-}* mesenchyme showed a significant loss of *Epha4*. EphA4 is one of 15 different Eph receptors that interact at the cell-cell interface with nine possible cell surface-bound ephrin ligands to serve diverse developmental functions, including axon repulsion and attraction (Eberhart et al., 2002; Kullander and Klein, 2002),

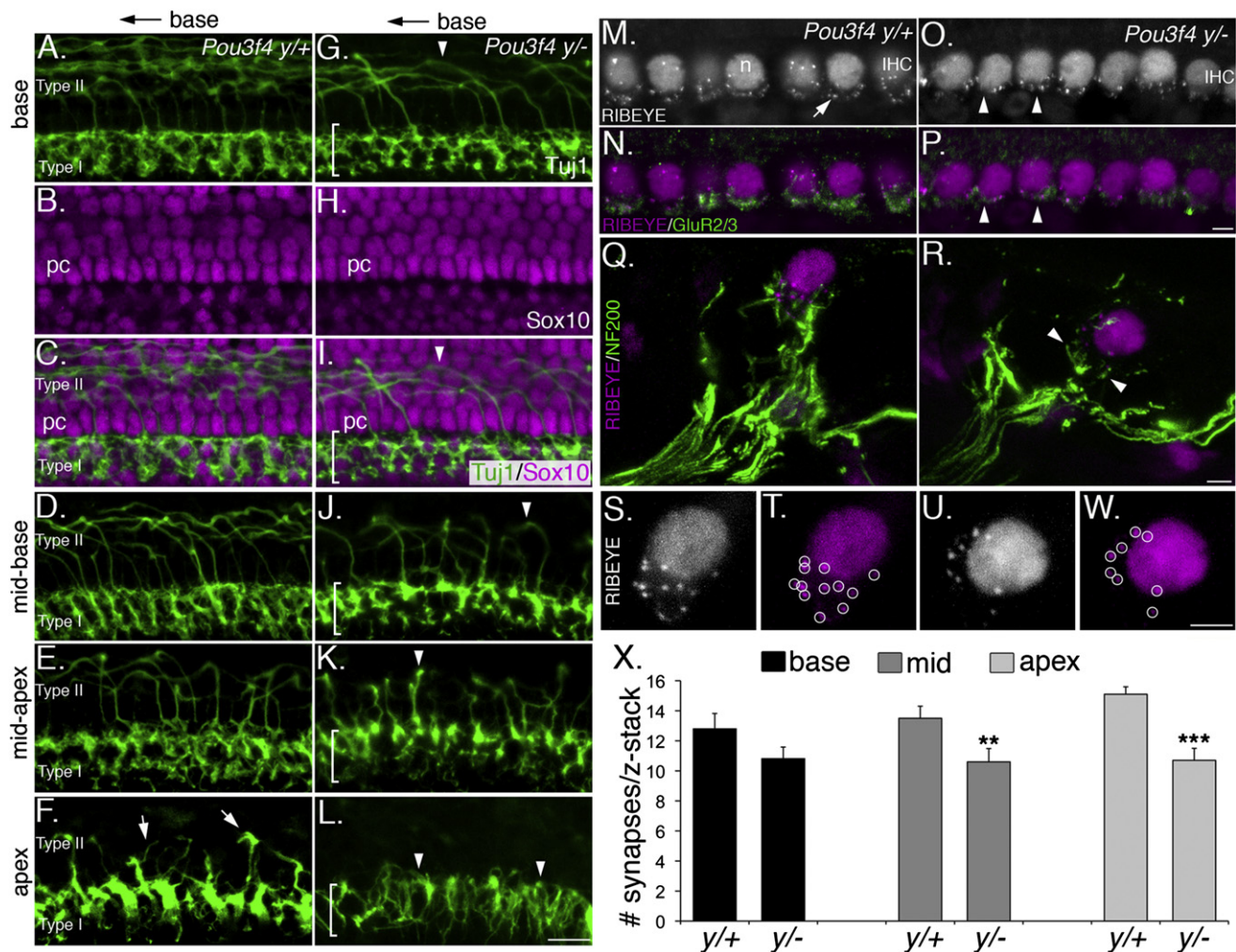


Figure 3. Defects in Fasciculation in *Pou3f4^{y/-}* Mice Impair Innervation and Synapse Formation

(A–L) Type I and type II projections in *Pou3f4^{y/+}* and *Pou3f4^{y/-}* embryos at E17.5. Only the distal 10 μ m of the type I fibers are shown. Scale bar in (L) represents 50 μ m.

(A–C) At the base of the cochlea, type I fibers innervate the inner hair cell layer, whereas type II fibers cross the pillar cell layer (shown in A and C) and then turn toward the base.

(D–F) Illustration of the base-to-apex gradient of maturation of type II fibers. At E17.5, type II projections are abundant in the midbase, sparse in the midapex, and short at the apex (arrows).

(G–I) In *Pou3f4^{y/-}* embryos at E17.5, the type I layer is less dense (see bracketed regions), and there are fewer type II projections (arrowheads).

(J–L) Compared with wild-type, *Pou3f4^{y/-}* embryos show fewer, less-mature type II projections. At the apex (L), no type II projections are observed. Scale bar represents 40 μ m.

(M–P) Whole-mount preparation of the apex of *Pou3f4^{y/+}* and *Pou3f4^{y/-}* cochleae at P8. Anti-Ribeye immunostaining indicates ribbon synapses (see arrow in M). This antibody also recognizes CtBp2 (n in all hair cell nuclei). IHC, inner hair cell. Anti-GluR2/3 in (N) indicates postsynaptic glutamate receptors. Immunostaining for both factors in the mutant appears reduced (arrowheads). Scale bar in (P) represents 8 μ m.

(Q and R) Midmodiolar cross-sections of the inner hair cell region from *Pou3f4^{y/+}* (Q) and *Pou3f4^{y/-}* (R) cochleae at E17.5. Nerve terminals are marked by anti-neurofilament (200 kDa). Note the decreased density of nerve fibers contacting the inner hair cell in *Pou3f4^{y/-}* (arrowheads). Scale bar in (R) represents 5 μ m.

(S and T) A high-magnification view of the synaptic region from the inner hair cell in (Q). Punctate spots (circled in T) represent individual ribbon synapses.

(U and W) Similar view as in (S) and (T) but from the *Pou3f4^{y/-}* inner hair cell in (R). Note the decreased number of ribbon puncta. Scale bar represents 4 μ m.

(X) Histogram indicating a significant decrease in the number of inner hair cell synapses (mean \pm SEM) in *Pou3f4^{y/-}* cochleae at P8. **p < 0.01; ***p < 0.001.

cooperative axon targeting (Gallarda et al., 2008), and axon fasciculation (Bossing and Brand, 2002; Orioli et al., 1996). Therefore, the developmental expression pattern of EphA4 in the cochlea was examined (Figures 4A–4F). Through the use of *in situ* hybridization, we found that *Epha4* mRNA is broadly

distributed at E14.5 (data not shown) and E16.5 (Figures 4A and 4B), localizing to mesenchyme, the spiral ganglion, and the cochlear epithelium. However, we saw a remarkably limited pattern of expression with antibodies specific to the extracellular domain of EphA4 protein: virtually all immunoreactivity was

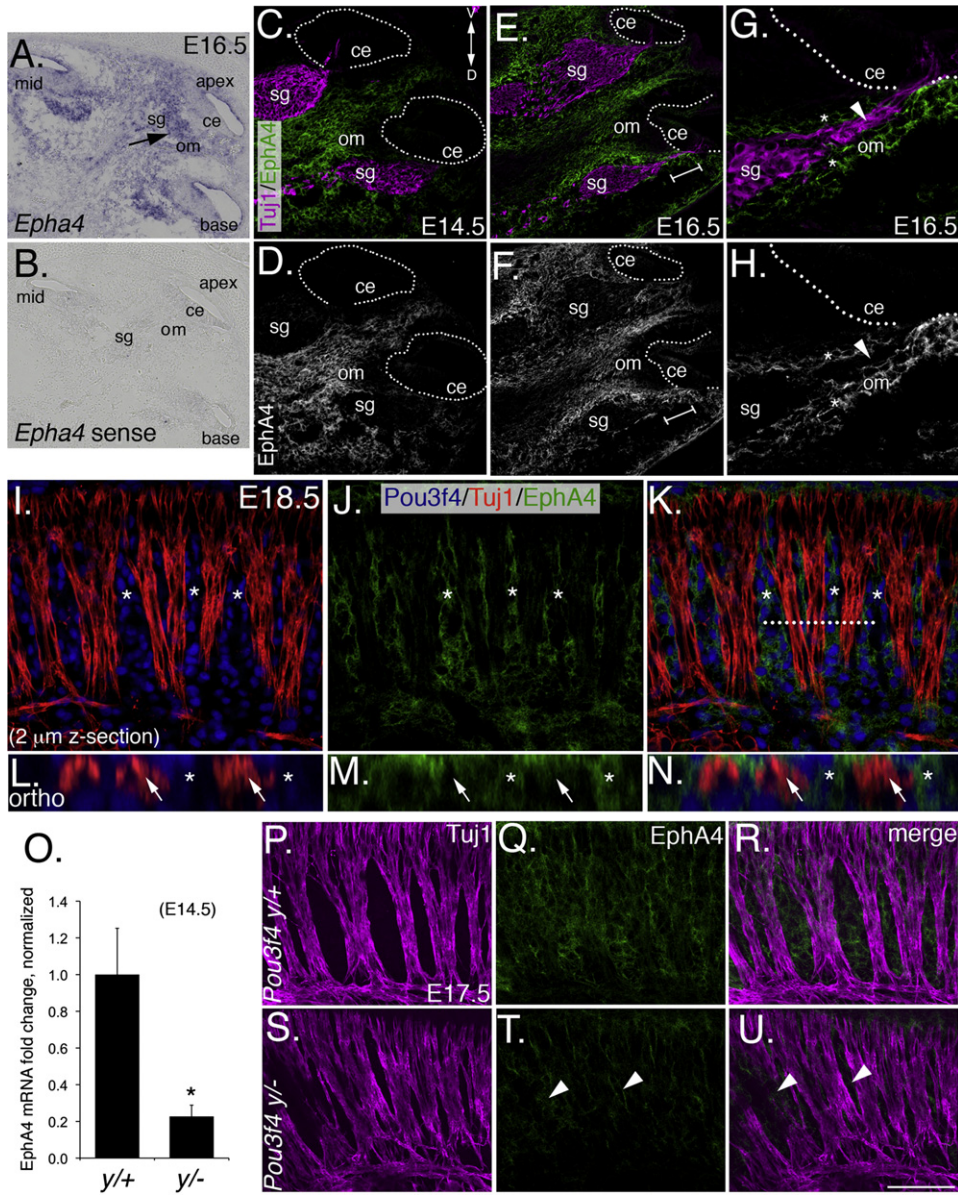


Figure 4. EphA4 Is Expressed in the Otic Mesenchyme during Development and Is Decreased in *Pou3f4^{y/-}* Embryos

(A and B) *Epha4* in situ hybridization in the E16.5 cochlea. (A) displays antisense and (B) shows sense. Sg, spiral ganglion; om, otic mesenchyme; ce, cochlear epithelium.

(C and D) EphA4 immunostaining at E14.5. Note the absence of EphA4 in all tissues except the otic mesenchyme. The dotted lines delineate the cochlear epithelia.

(E–H) EphA4 immunostaining at E16.5. (G) and (H) are a high-magnification view of the bracketed regions in (E) and (F). Note the “guide rails” marked by the asterisks and the absence of EphA4 staining in the SGN axons (arrowheads).

(I–K) Whole-mount preparation of a cochlea at E18.5. EphA4 expression is restricted to the mesenchyme (asterisks).

(L–N) Orthogonal confocal reconstructions from the dotted line in (K).

(O) Quantitative PCR data showing that *EphA4* expression levels are reduced approximately 5-fold in otic mesenchyme from *Pou3f4^{y/-}* embryos (mean ± SEM). *p ≤ 0.05.

(P–U). EphA4 expression in wild-type and *Pou3f4^{y/-}* embryos (where it is reduced; see arrowheads) in whole mount at E17.5.

For (A) and (B), the scale bar in (U) represents 120 μm; for (C)–(F), the scale bar in (U) represents 100 μm; for (G)–(K), the scale bar in (U) represents 50 μm; for (L)–(N), the scale bar in (U) represents 15 μm; for (P)–(U), the scale bar represents 70 μm.

observed in otic mesenchyme cells (Figures 4C–4F). A high-magnification view of the SGN peripheral axons (Figures 4G and 4H) shows that EphA4 protein is expressed only by the

adjacent mesenchyme cells in a “guide rails” fashion (see asterisk, Figures 4G and 4H) but is not detectable in the SGN axons (arrowheads) themselves. Importantly, whole-mount

preparations and orthogonal reconstructions of E18.5 cochleae show that EphA4 is distributed in the Pou3f4-positive mesenchyme bands between the SGN fascicles but does not overlap with Tuj1 (Figures 4I–4N). These results indicate that EphA4 protein is distributed in a spatial and temporal manner consistent with a role in SGN fasciculation. It is unclear why there is a discrepancy between EphA4 mRNA and protein distribution, but a posttranscriptional regulatory program that limits EphA4 protein to the mesenchyme may be present.

To confirm that EphA4 expression in the mesenchyme depends on *Pou3f4*, we used quantitative PCR to show an approximate 5-fold reduction in *Epha4* expression in *Pou3f4^{y/-}* cochleae (Figure 4O). Moreover, analyses of whole-mount preparations from *Pou3f4^{y/-}* cochleae show that EphA4 protein is substantially reduced in the otic mesenchyme at E17.5 (Figures 4P–4U).

EphA4 Promotes SGN Fasciculation and Hair Cell Innervation

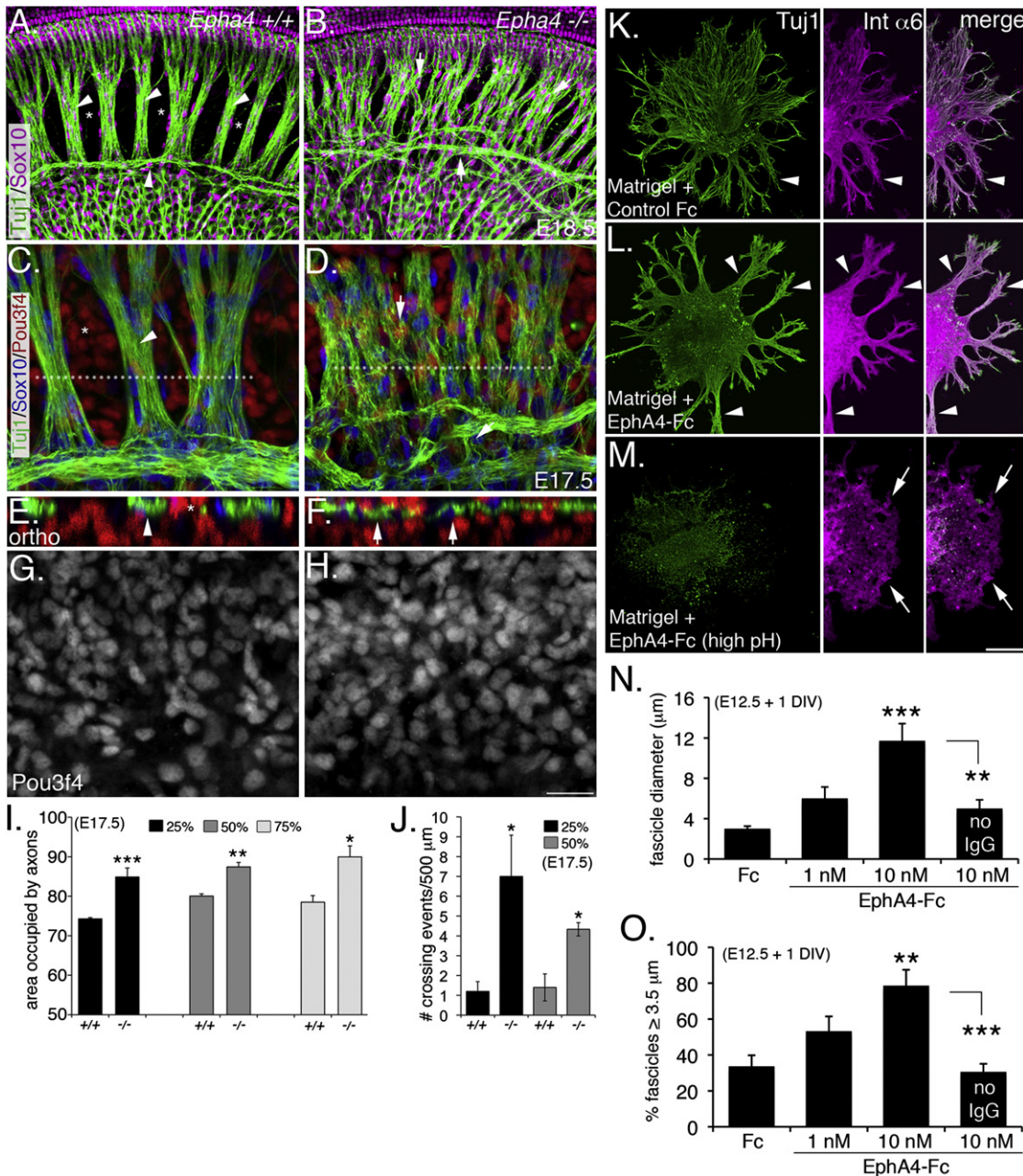
If *Pou3f4* transcriptional activity regulates *Epha4* expression in the otic mesenchyme to promote SGN fasciculation, we reasoned that *Epha4*-deficient mice should also have fasciculation defects. We therefore examined the SGNs from *Epha4^{-/-}* embryos at late embryonic ages (Helmbacher et al., 2000; North et al., 2009). Compared to their wild-type littermates (Figures 5A, 5C, 5E, and 5G), *Epha4^{-/-}* mice presented fasciculation defects that were remarkably similar to those observed in the *Pou3f4^{y/-}* animals (Figures 5B, 5D, 5F, and 5H; compare to Figure 2). Whereas wild-type cochleae showed tight SGN bundles and well-defined mesenchyme bands (Figures 5A and 5C), the SGNs in *Epha4^{-/-}* cochleae displayed dispersed, poorly fasciculated bundles that aberrantly traversed the mesenchymal space (Figures 5B and 5D) and occupied significantly more area at the basal, midmodiolar, and apical regions of the cochlea (Figure 5I). Orthogonal reconstructions of these samples illustrate disruptions in the normal interdigititation of the mesenchyme cells and the SGN bundles in the *Epha4^{-/-}* mutants (Figures 5E and 5F). The number of mesenchyme cells in *Epha4^{-/-}* cochleae appeared unchanged compared to wild-type, suggesting that the fasciculation defects in the SGNs are not due to a loss of surrounding mesenchyme (Figures 5G and 5H). Similar to SGNs from *Pou3f4^{y/-}* mice, SGNs from *Epha4^{-/-}* mice showed an approximately 4-fold increase in the number of axons that crossed between bundles (Figure 5J). Finally, we examined *Epha4^{-/-}* cochleae at P7 to determine whether these animals (like *Pou3f4^{y/-}* mice) had defects in hair cell innervation and ribbon synapse formation (Figure S2). As a result of early postnatal lethality of this line, we were only able to examine four mutant ears, and thus our conclusions are based on a limited sampling. Compared to controls (Figures S3A, S3C, and S3D), *Epha4^{-/-}* mice showed a nearly 2-fold reduction in the number of ribbon synapses (Figures S2B, S2E, and S2F), further supporting that SGN fasciculation is important for target innervation. Overall, the fasciculation and synapse defects in *Epha4* and *Pou3f4* mutants are very similar, consistent with their participation in a common developmental process.

To investigate whether EphA4 plays a non-cell-autonomous role during SGN fasciculation, we asked whether exogenous

EphA4 extracellular domains (serving as a substitute for mesenchyme) could promote SGN fasciculation in vitro. E12.5 spiral ganglia were cultured for 24 hr (without otic mesenchyme) on a layer of Matrigel infused with either control Fc or EphA4-Fc (Figures 5K–5M) to determine the effects on fasciculation. We also examined the effects of preclustering EphA4-Fc to determine whether “activating” (preclustered form) or “blocking” (unclustered form) ephrin ligands on the SGNs had different effects on fasciculation (Davis et al., 1994). In the presence of control Fc (preclustered), SGN explants projected mostly single neurites and some rudimentary fascicles (Figure 5K, see arrowheads), suggesting that SGNs may have some intrinsic axoaxonal binding capacity. However, explants cultured with preclustered EphA4-Fc showed dramatically enhanced fasciculation, with thick bundles projecting away from the soma (Figure 5L) and very few single neurites. Interestingly, EphA4-Fc treatments did not reduce the length of axons (growth cone collapse) compared to controls (data not shown). When we stained these cultures with anti-integrin- $\alpha 6$ antibodies to mark the auditory glia, we found their growth pattern to be almost identical to that of the SGNs, raising the possibility that the glia may also respond to EphA4. However, when the SGNs were eliminated in the presence of high pH culture medium (Mukai et al., 2011) but grown in preclustered EphA4-Fc, the glia persisted but did not bundle (Figure 5M), suggesting that SGN fasciculation is not normally a secondary response to aggregating glia. Preclustered EphA4-Fc at 10 nM led to a 4-fold increase in average bundle diameter compared to controls (Figure 5N) and doubled the percentage of fascicles greater than 3.5 μm in diameter (Figure 5O). Importantly, cultures grown in the presence of unclustered EphA4-Fc showed levels of bundling that were not significantly different from controls (see Figures 5N and 5O), suggesting that blocking ephrins from recognizing Eph receptors on neighboring axons or glia has little effect on SGN fasciculation. These results demonstrate that EphA4, expressed by mesenchyme cells, may normally activate ephrin ligands expressed by SGNs to promote fasciculation.

Pou3f4 Knockdown In Vitro Causes SGN Fasciculation Defects that Are Rescued by EphA4

To determine whether *Pou3f4* and EphA4 are functionally linked, we established an in vitro system to investigate SGN fasciculation using explanted SGNs and otic mesenchyme. At E12.5, the auditory component of the cochleo-vestibular ganglion can be easily isolated and cocultured with pieces of otic mesenchyme; over time these cell populations intercalate, while developing SGNs extend processes (Figure 6A; Figure S3). In these assays, the SGNs appear to briefly migrate away from the explant and then extend axons (often in clusters with other neurons; see Figure S3) at the same time that mesenchyme cells invade. In addition, coculturing the SGNs and mesenchyme in a thick Matrigel layer allows the two cell populations to interact in a semi-three-dimensional gel, mimicking SGN fasciculation in vivo (Figures S3B and S3C). To examine the effects of decreased expression of *Pou3f4*, we used Morpholino antisense oligonucleotides (MOs) to knock down *Pou3f4*. Figure 6A shows uptake of a control MO-fluorescein isothiocyanate (FITC) conjugate by endocytic vesicles in mesenchyme and neurons.

**Figure 5. EphA4/EphA4 Promotes SGN Fasciculation and Hair Cell Innervation**

(A and B) Wild-type (A) and *EphA4*^{-/-} (B) cochleae at E18.5. Arrowheads in (A) point to well-defined SGN fascicles, and asterisks mark normally formed bands of mesenchyme. In contrast, less SGN fasciculation and axons inappropriately traverse the mesenchyme (arrows) in the *EphA4*^{-/-} cochlea (B).

(C and D) High-magnification views of wild-type (C) and *EphA4*^{-/-} (D) cochleae at E17.5 illustrating how the SGNs fail to bundle.

(E and F) Orthogonal reconstructions from the regions marked by dotted lines in (C) and (D) showing that the SGN bundles and mesenchyme are no longer segregated.

(G and H) Monochrome images indicate no change in Pou3f4 expression in *EphA4*^{-/-} cochleae.

(I and J) Histograms illustrate the axon fasciculation defects (I) and the number of times per 500 μm that individual processes crossed between fascicles (J). Percentages indicate the position along the length of the cochlea with respect to the distance from the base. **p ≤ 0.01; ***p ≤ 0.001.

(K and L) E12.5 SGN explants cultured for 24 hr in the presence of Matrigel + Fc control or Matrigel + EphA4-Fc (both preclustered forms). The middle panels show the auditory glia (Int α6 positive).

(M) Same as (L), but the neurons were eliminated using high pH culture medium.

(N and O) Histograms showing increased fascicle diameter (N) and percentage of large (≥ 3.5 μm) fascicles in response to EphA4-Fc. **p ≤ 0.01; ***p ≤ 0.001.

For (A) and (B), the length of the scale bar in (H) represents 50 μm; for (C), (D), (G), and (H), the length of the scale bar in (H) represents 20 μm; for (E) and (F), the length of the scale bar in (H) represents 15 μm. The scale bar in (M) represents 100 μm. DIV indicates days in vitro. Mean ± SEM for (I), (J), (N), and (O).

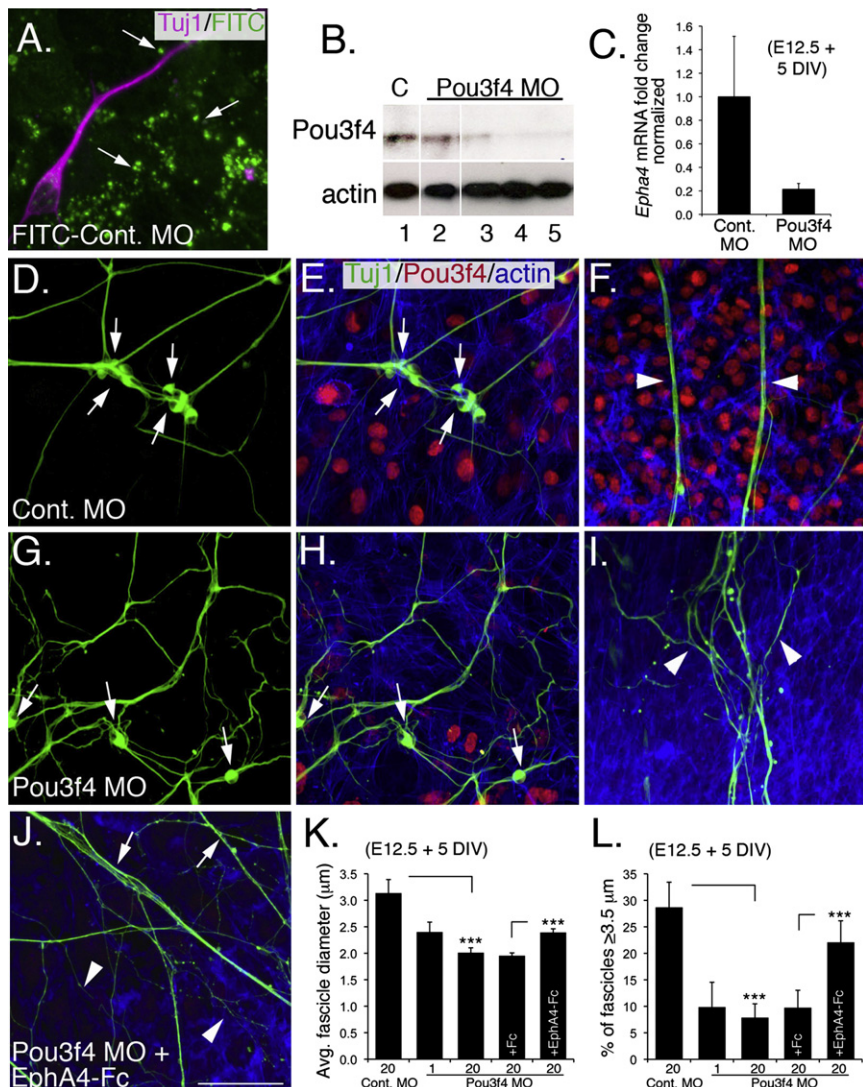


Figure 6. Exogenous EphA4 Protein Rescues Pou3f4-Dependent Fasciculation Defects In Vitro

(A) Coculture of SGNs (purple) and mesenchyme cells. Punctate FITC-labeling indicates uptake of FITC-conjugated control MO by endocytic vesicles.

(B) Western blot demonstrating knockdown of endogenous Pou3f4 by a Pou3f4 MO. Lane 1, 20 μM control MO; lane 2, 1 μM Pou3f4 MO; lanes 3–5, three different samples treated with 20 μM Pou3f4 MO. Anti- β -actin, loading control.

(C) Quantitative PCR demonstrates a 5-fold reduction of *Epha4* transcripts in mesenchyme cells treated with the Pou3f4 MO.

(D–J) SGN and otic mesenchyme cocultures treated with indicated MO. Green, anti-Tuj1 (neurons); red, anti-Pou3f4; blue, phalloidin (actin). (D–F) In the presence of 20 μM control MO, SGN cell bodies cluster (arrows in D and E) and have axons that form thick, straight fascicles that extend away from the cell bodies (arrowheads in F).

(G–I) Treatment with 20 μM Pou3f4 MO decreases clustering of cell bodies (arrows in G and H) and decreases axon fasciculation (arrowheads in I). In addition, individual fibers follow more convoluted paths. Knockdown of Pou3f4 is illustrated in (H).

(J) Treatment with 20 μM Pou3f4 MO + 10 nM EphA4-Fc increases incidences of thick, straight fascicles (arrows), although single nonfasciculated neurites are still present (arrowheads). For panel (A), the scale bar in (J) represents 20 μm ; for (D)–(J), the scale bar in (J) represents 40 μm .

(K and L) Histograms illustrating changes in average fascicle diameter (μm) and average percentage of large ($\geq 3.5 \mu\text{m}$) fascicles among the different treatment groups. *** $p \leq 0.001$. Mean \pm SEM for (C), (K), and (L).

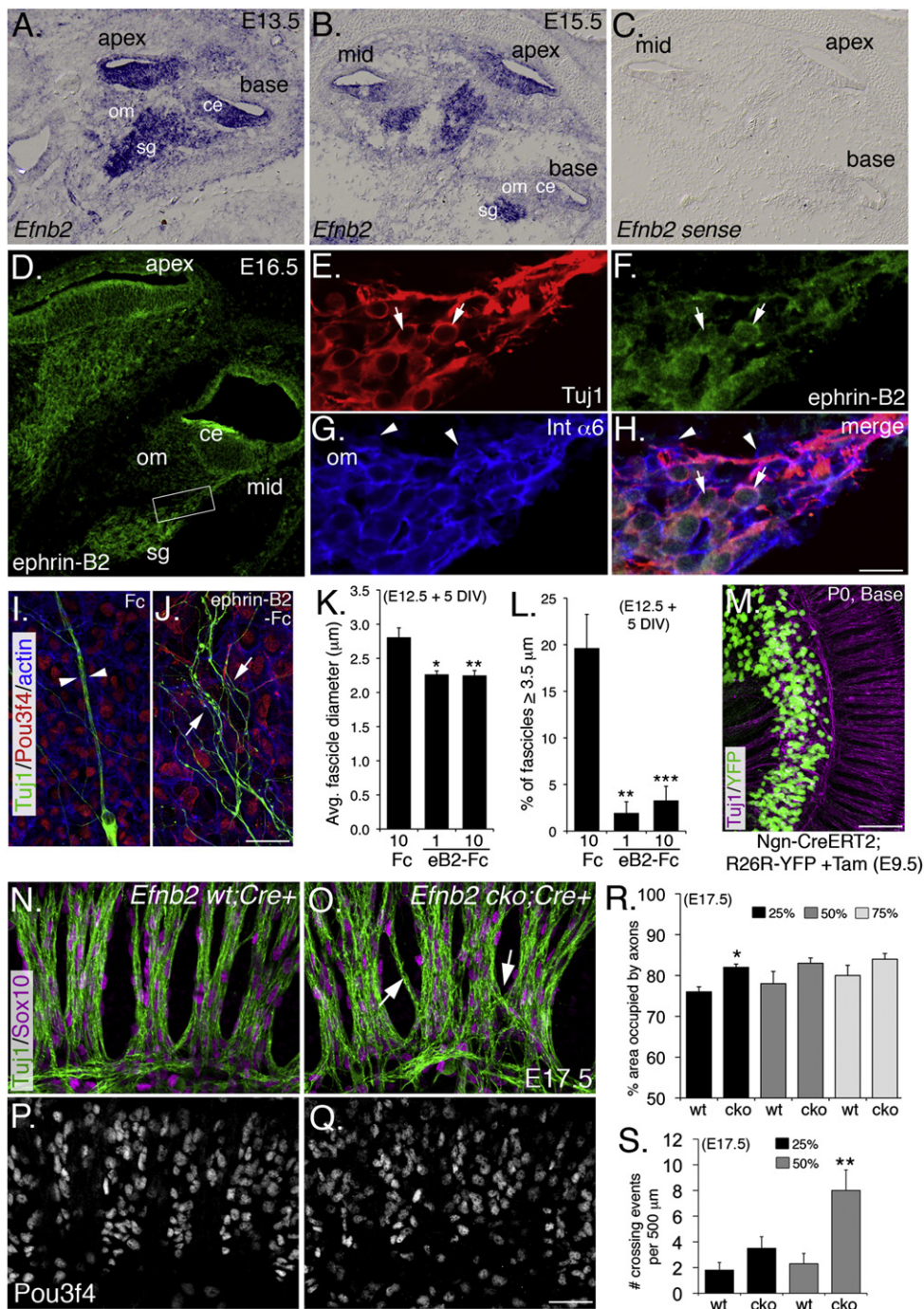
A Pou3f4-specific antisense MO at 20 μM showed a nearly complete knockdown of Pou3f4 (Figure 6B). Treatment with the Pou3f4 MO also induced a significant knockdown of *EphA4* (Figure 6C), confirming a direct effect for Pou3f4 on *EphA4* expression.

The soma of SGNs maintained in coculture with control MO were typically clustered with one another (Figures 6D and 6E), and their neurites often formed extensive and straight fascicles that extended through the mesenchyme cells (Figure 6F; Figure S3) (Simmons et al., 2011). In contrast, when cultures were treated with the Pou3f4 MO, SGNs failed to form clusters (Figures 6G and 6H). Distal processes still extended among the otic mesenchyme cells, but these processes failed to fasciculate and often followed more tortuous paths (Figure 6I), similar to *Pou3f4*^{y−} cochleae. To quantify these effects, we determined average SGN fascicle diameter for both conditions. In controls, average fascicle diameter was approximately 3.1 μm (Figure 6K; individual SGN neurites in culture are small, typically $\sim 1 \mu\text{m}$ in diameter), and 28% of fascicles were classified as large fascicles

(larger than or equal to 3.5 μm ; Figure 6L). Fascicles in Pou3f4 MO-treated cultures had a significantly smaller average diameter of 2 μm , and only 8% of the fascicles were classified as large (Figure 6L). To determine whether fasciculation loss was a result of downregulating *EphA4*, we added EphA4-Fc protein to SGN and mesenchyme cultures that had been treated with the Pou3f4 MO. The addition of preclustered EphA4-Fc restored SGN fasciculation (Figure 6J) and induced a statistically significant increase in fascicle diameter size, as well as a 12% enhancement of large fascicles (Figures 6K and 6L).

Ephrin-B2 Acts as a Cofactor for EphA4 during SGN Fasciculation

We next reasoned that if EphA4 expression by otic mesenchyme cells promotes SGN fasciculation, then at least one ephrin cofactor must be expressed by the SGNs. Thus, an extensive *in situ* hybridization survey was performed to determine which of the seven known EphA4 ligands (Wilkinson, 2001) are expressed by SGNs during mid-to-late gestation (Figure S4;

**Figure 7. Ephrin-B2 Acts as a Cofactor for EphA4 during SGN Fasciculation**(A–C) *Efnb2* *in situ* hybridization at E13.5 and E15.5. sg, spiral ganglion; ce, cochlear epithelium; om, otic mesenchyme.

(D) Ephrin-B2 antibody staining of the cochlea at E16.5.

(E–H) High-magnification view from the boxed region in (D) shows SGNs (E), ephrin-B2 expression primarily in the neurons (F, see arrows), glial cells (G, see arrowheads), and merge (H).

(I and J) Representative control Fc and ephrin-B2-Fc-treated samples from SGN and otic mesenchyme cultures. See main text for details.

(K and L) Histograms showing decreased average fascicle diameter (K) and percentage of large fascicles (L) in the presence of blocking ephrin-B2-Fc.

(M) Tamoxifen induction of Ngn-Cre^{ERT2} induces expression of YFP reporter activity in ~95%–100% of SGNs (see Experimental Procedures).(N) Micrograph showing morphology of the radial bundles in a control *Efnb2 wt; Cre+* cochlea.(O) Micrograph showing less fasciculation and fewer processes crossing between bundles (arrows) in *Efnb2 cko; Cre+* cochlea.(P and Q) Pou3f4 staining shows that mesenchyme is normal in both WT and *Efnb2 cko* cochleae.

Figure 7). For *Efna1*, *Efna5*, and *Efnb3*, mRNA was not detectable at appreciable levels in the cochlea (data not shown). Transcripts for both *Efna2* and *Efna4* were distributed broadly in the cochlea, including the spiral ganglion, and *Efna3* appeared in the SGNs but at a level just slightly above the control probe (**Figure S4**). In contrast, *Efnb2* was detected at high levels in SGNs at E13.5 (**Figure 7A**) and at E15.5, when SGN fasciculation commences (**Figures 7B** and **7C**). Ephrin-B2 protein was similarly detected in the SGNs and their axons by immunostaining (**Figure 7D**) and overlapped primarily with neuronal markers (Tuj1; **Figures 7E**, **7F**, and **7H**, see arrows), but not with markers of auditory glia (integrin- α 6; **Figures 7G** and **7H**, see arrowheads). The complementary expression of ephrin-B2 on SGN axons and EphA4 on adjacent mesenchyme (compare **Figure 7D** to **Figure 4F**) suggested that ephrin-B2 is spatially and temporally positioned to interact with EphA4 during SGN fasciculation.

We next predicted that if EphA4 signals through ephrin-B2 in this system, then blocking ephrin-B2 function using unclustered ephrin-B2-Fc would prevent SGN fasciculation in SGN and mesenchyme cocultures, similar to the effects of the Pou3f4 MO. Consistent with this hypothesis, ephrin-B2-Fc led to a nearly 25% decrease in fascicle diameter and a >4-fold decrease in the number of large fascicles, as compared to control (**Figures 7I**–**7L**). We next asked whether the loss of *Efnb2* in the SGNs *in vivo* would lead to fasciculation defects similar to those observed in the *Pou3f4* and *EphA4* mutants. Because *Efnb2* was detectable in regions of the cochlea besides the SGNs, particularly at earlier stages (**Figures 7A**, **7B**, and **7D**), we conditionally removed *Efnb2* in the SGNs by crossing *Efnb2 loxP* mice (Gerety and Anderson, 2002) to mice carrying *Ngn-CreERT2* (Koundakjian et al., 2007), a transgene that shows robust reporter activity in the SGNs after tamoxifen delivery (**Figure 7M**). Resulting *Efnb2* conditional knockout (cko) mice showed substantially reduced levels of ephrin-B2 protein, particularly in the SGN peripheral axons (**Figure S4**), but not in other regions of the cochlea.

Compared to Cre-positive wild-type littermate controls (**Figures 7N** and **7P**), the SGNs from *Efnb2 cko* cochleae showed both fasciculation defects and axons that aberrantly crossed between fascicles but did not show a loss of mesenchyme (**Figures 7O** and **7Q**). Although statistically significant in some cases, these defects were less severe compared to what we observed in the *Pou3f4* or *EphA4* mutants, probably owing to functional redundancy by other ephrins present or possibly a lack of complete ephrin-B2 elimination. *Efnb2 cko* cochleae showed a 6% increase in area consumed by axons and maximally a 4-fold increase in the number of axons that crossed between bundles (**Figures 7R** and **7S**). Because tamoxifen was given at a single dose at E9.5–E10.5, most defects were observed at the base and midmodiolar regions of the cochlea, in accordance with previous studies with *Ngn-CreERT2* (Koundakjian et al., 2007). Importantly, the *Efnb2 cko* phenotype was similar to the fasciculation phenotypes observed in both the

Pou3f4 and *EphA4* mutants lines, suggesting that ephrin-B2 may function as a ligand for EphA4 in this process.

Pou3f4 Associates with EphA4 Regulatory Elements

We next asked whether, in the developing otic mesenchyme, regulatory elements of *EphA4* are a direct target of Pou3f4. Pou proteins are known to have a bipartite DNA binding system that includes a POU-specific domain, as well as a homeobox domain (Phillips and Luisi, 2000). Whereas the recognition sequences of several Pou proteins have been characterized, relatively little is known about mouse Pou3f4. However, one report has demonstrated that Pou3f4 preferentially recognizes the tandem homeobox sequence ATTATTA in the regulation of the dopamine receptor 1A gene *D1A* (Okazawa et al., 1996). Therefore, we scanned the entire *EphA4* genomic sequence and found four of these sites within introns in the first 70 kilobases (kb) and one approximately 8.5 kb upstream of exon 1 (**Figure 8A**). We then performed chromatin immunoprecipitation (ChIP) using otic mesenchyme and a Pou3f4-specific IgY and assayed the resulting DNAs for these *EphA4* regulatory regions using quantitative PCR (**Figure 8B**). In these experiments β -actin, *Neurogenin-1*, and an *EphA4* site that did not contain ATTATTA were used as negative controls; there was no significant association at these sites with the control or Pou3f4-specific IgY. However, all five of the putative *EphA4* regulatory regions showed preferential association (with statistical significance) with the Pou3f4-specific IgY, with little to no association with the control IgY (**Figure 8B**). These data suggest that Pou3f4 may directly regulate *EphA4* in otic mesenchyme cells in order to initiate EphA4-mediated SGN fasciculation.

DISCUSSION

The results presented in this study reveal a new and intriguing role for otic mesenchyme in the development of cochlear innervation. Moreover, the identification of additional auditory defects arising from the absence of *Pou3f4* provides insights into the underlying basis for the deafness that occurs in both human and murine mutants. Previous reports have demonstrated a significant decrease in endocochlear potential that is almost certainly a major component of the auditory dysfunction, but the demonstration of a 30% decrease in the number of ribbon synapses may indicate a significant loss in acuity. Although this hypothesis cannot be tested without a mouse model in which endocochlear potential is preserved, it would need to be considered in terms of developing any potential therapeutic interventions.

The results presented here identify a molecular signaling pathway in which Pou3f4 expression in otic mesenchyme cells directly activates *EphA4*, leading to the expression of EphA4 on the surface of these cells (**Figure 8C**). The presence of EphA4 provides a cue that acts, along with the spatial distribution of

(R and S) Histograms illustrating axon fasciculation defects (R) and the number of times per 500 μ m that individual processes crossed between fascicles (S). Percentages indicate the position along the length of the cochlea with respect to the distance from the base. *p \leq 0.05; **p \leq 0.01. For (A)–(C), the length of the scale bar in (H) represents 200 μ m; for (D), the length of the scale bar in (H) represents 100 μ m; for (E)–(H), the length of the scale bar represents 20 μ m. The scale bar in (J) represents 40 μ m. The scale bar in (M) represents 80 μ m. The scale bar in (Q) represents 40 μ m. Mean \pm SEM for (K), (L), (R), and (S).

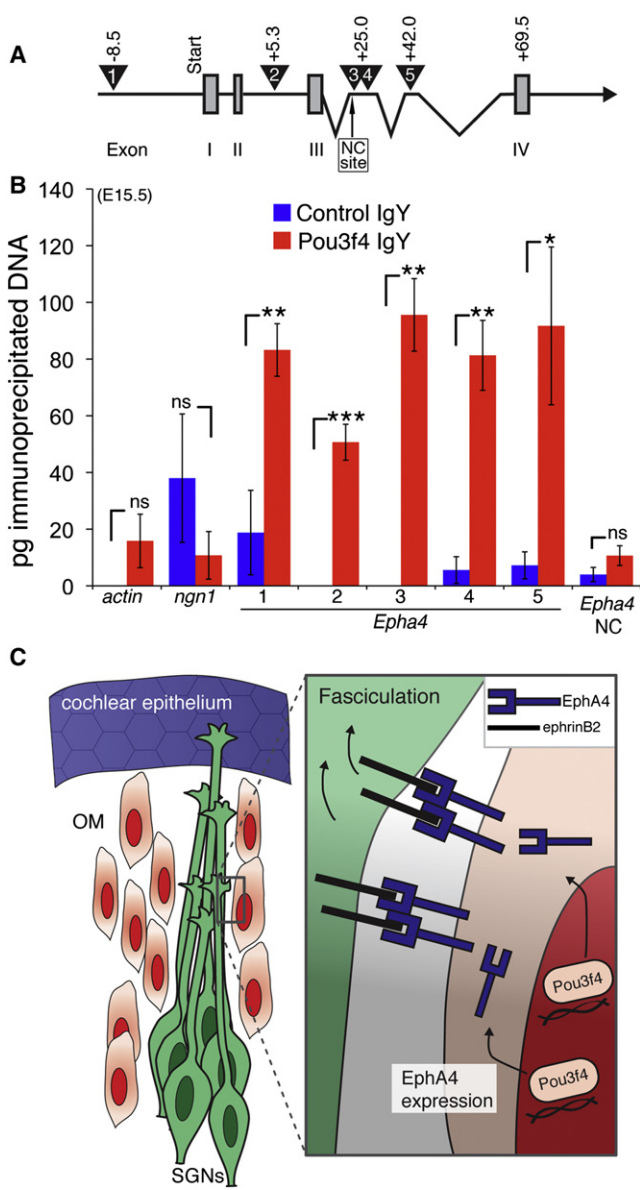


Figure 8. Pou3f4 Protein Associates with EphA4 Regulatory Elements

(A) A cartoon schematic of *EphA4* showing the first four of 16 exons. Exons I–IV are represented by numbered gray boxes. The numbered triangles indicate the regions containing the putative Pou3f4 binding site ATTATTA. Primer sets were designed to amplify these five regions after ChIP. NC site, the negative control site.

(B) Histogram showing the number of picograms (pg) of immunoprecipitated chromatin for each primer set. ns, not significant. *p ≤ 0.05; **p ≤ 0.01; ***p ≤ 0.001. Mean ± SEM.

(C) Cartoon schematic of a proposed model. Pou3f4 in otic mesenchyme induces expression of *EphA4/EphA4*, which binds to ephrin-B2 on developing SGN axons, leading to fasciculation. As a result, SGN axons fasciculate to give rise to the inner radial bundles.

otic mesenchyme, to promote fasciculation of SGNs via binding to ephrin-B2 on their surfaces. Furthermore, these data predict that EphA4 activates ephrin-B2 to generate a reverse

signaling response to segregate the SGNs and mesenchyme in a manner classically documented in zebrafish animal cap assays (Mellitzer et al., 1999). However, the mechanism(s) by which ephrin-B2 promotes fasciculation among the SGN axons remains unclear. Ephrin-B2 reverse signaling may induce filopodial collapse (Cowan and Henkemeyer, 2001) by the SGN growth cones, which, by default, may lead them to preferentially associate with neighboring axons. Or ephrin-B2 reverse signaling may promote SGN interaxonal adhesion by signaling to other cell-surface factors known to regulate fasciculation, such as IgCAMs (Lin et al., 1994) and/or integrins (Baum and Garriga, 1997).

These results reveal the molecular basis for the organizing effects of otic mesenchyme and show a paracrine mode of action for Pou3f4 in axon guidance. Interestingly, Pou4F2 (Brn3b) is known to regulate axon pathfinding and fasciculation in retinal ganglion cells through an autocrine signaling pathway (Pan et al., 2008), and in *Drosophila*, deletion of the *Pou3f4* ortholog *ventral veins lacking* (*vvl*) leads to defects in fasciculation and steering of axons in the fly brain, although much of these defects may be secondary to effects on neuronal specification (Meier et al., 2006). In addition, although this demonstrates a role for Eph-ephrin signaling in the initial development of the peripheral auditory system, elegant work by Huffman and Cramer (2007) has already demonstrated a role for EphA4 in hearing and central auditory plasticity (Hsieh et al., 2007; Huffman and Cramer, 2007). These authors showed that, after surgically removing the cochlea (and peripheral input to the brain), the expression of *EphA4* was critical for target selection during remodeling (Hsieh et al., 2007; Miko et al., 2008). The functions of ephrin-Eph receptor interactions probably go well beyond those presented here and in previous publications. As shown in Figure S4 and in previous reports, several other ephrins and Ephs are expressed in the cochlea (Bianchi and Gale, 1998; Zhou et al., 2011) and may serve a variety of additional functions. This may also indicate why EphA4-Fc was only able to partially rescue the fasciculation defects in the absence of Pou3f4 (Figure 6). In particular, axon-axon interactions by Ephs and ephrins may also play a role in SGN radial bundle formation, similar to the coordinated actions of motor and sensory axons, as has been shown recently (Gallarda et al., 2008; Wang et al., 2011). Indeed, when cultured in the absence of mesenchyme, SGNs have some intrinsic capacity to fasciculate. Inhibiting ephrins expressed on SGNs with unclustered EphA4-Fc did not diminish fasciculation compared to controls (Figure 5), but a more complete characterization of other Eph-ephrin interactions would be required to eliminate this possibility.

The innervation patterns of the mammalian auditory system are remarkably complex, containing multiple fiber and bundle types (reviewed in Appler and Goodrich, 2011). Despite a wealth of descriptive and functional studies beginning as early as the late 1800s, the specific functions of different fiber tracts and neuronal cell types are only now being elucidated. Mutations in *Pou3f4*, *EphA4*, or *Efnb2* lead to defects in the formation of radial fiber bundles, but the functions of these bundles are unknown. Considering their regular alignment along the tonotopic axis of the cochlea, it has been suggested that each bundle may contain fibers tuned to a specific frequency and that radial bundle

formation may thus play an important role in coordinating frequency matching between SGNs and auditory hair cells (Ruebel and Fritzsch, 2002). If this is the case, then defects in radial bundle formation, such as those reported in this study, could lead to significant tonotopic defects in the cochlea and possibly higher CNS auditory nuclei. This conclusion is supported by the significant functional and morphological defects in the auditory systems of *Epha4* and *Efnb2* mutant mice (Miko et al., 2008), with auditory brainstem response waveform signatures suggesting defects both peripherally and centrally. Unfortunately, the direct roles of EphA4 and ephrin-B2 in the formation of tonotopic organization in the auditory brainstem make it impossible to discern the specific effects of defects in radial bundle formation without generating inner-ear-specific mutants.

The increased number of crossing fibers and the decrease in ribbon synapses observed in *Pou3f4/Epha4/Efnb2* mutants indicate that fasciculation signals arising from surrounding otic mesenchyme clearly act to prevent routing errors within the mesenchymal space by driving SGN fibers onto existing radial bundles. Previous studies indicated that otic mesenchyme cells express EphA4 protein (Pickles et al., 2002; van Heumen et al., 2000) and that EphA4 prevented outgrowth of mature SGNs in vitro (Brors et al., 2003). However, the results presented here demonstrate that for immature SGNs, rather than inhibiting axon outgrowth, EphA4/ephrin-B2 interactions act to form a barrier that promotes SGN fasciculation without affecting outgrowth. Overall, the factors that guide SGN axons during their pathfinding remain unknown. Neurotrophin signaling through TrkB and TrkC, although critical for growth and maintenance of SGNs, is not required for the directed outgrowth of SGNs (Fekete and Campero, 2007; Fritzsch et al., 2005). Additional studies will clearly be required to identify the neurotropic factors for SGNs.

EXPERIMENTAL PROCEDURES

Animal Care and Tissue Preparation

All animals used in this study were maintained in accordance with the National Institutes of Health (NIH) Care and Use Committee. Timed pregnant CD1 mice (Charles River Laboratories) were used for protein expression studies and neuron and mesenchyme explant cultures. *Pou3f4* mutant mice, in which the coding region was replaced with Cre recombinase, were maintained on a mixed background. This line phenocopies a previously published *Pou3f4* knockout mouse (Phippard et al., 1999). Because *Pou3f4* is on the X chromosome, only males were used in this study in order to avoid variability arising from X inactivation. In order to generate hemizygous males, we crossed *Pou3f4^{+/−}* females to wild-type CD1 males. To generate conditional *Efnb2* knockout animals (*Efnb2 cko*), we bred C57/BL6 *Efnb2 flox/flox* mice (Gerety and Anderson, 2002) with mice carrying the *Neurogenin (Ngn)-CreERT2* transgene (Koundakjian et al., 2007) on a mixed CD1 background. *Ngn1^{CreERT2}; Efnb2^{flox/+}* mice were crossed, and pregnant dams were gavaged with a single dose of tamoxifen (Sigma; solubilized in flax and sunflower seed oil; 0.5 mg/40 g body weight) at 9.5–10.5 days gestation. Through the use of this strategy, we found Cre reporter activity in 95%–100% of SGNs at the cochlear base (R26R-YFP; Jackson Laboratory; Figure 7).

Immunostaining and In Situ Hybridization

For whole-mount immunostaining of the SGNs, we isolated cochleae from the vestibular components, bony capsule, and associated stria. Following permeabilization with 0.5% Triton X-100 and blocking with 10% serum, the cochleae were incubated overnight at 4°C in primary antibodies and then rinsed extensively. Fluorescent secondary antibodies (Invitrogen, 1:1,000)

were applied for 1 hr at room temperature. For culture explants and cryoprotected tissue sections, we performed antibody staining as described previously (Driver et al., 2008). Confocal z stack images were obtained using an LSM-510 (Zeiss), projected using NIH-ImageJ, and then further processed using Adobe Photoshop. *In situ* hybridization was performed as described (Raft et al., 2007). For all templates, sense controls were generated in parallel. Tissue processing, sectioning, hybridization, and detection were performed as previously described (Raft et al., 2007).

Neuron and Mesenchyme Culture Experiments

CD1 embryos were prepared for culture experiments as described previously (Montcouquiol et al., 2003). Culture medium included Dulbecco's modified Eagle's medium, 10% fetal bovine serum, 0.2% N2, and 0.001% ciprofloxacin. In pilot experiments, we determined that the spiral ganglion persisted in culture up to 5 days without additional neurotrophins only if the glia were not removed. For the 24 hr Matrigel outgrowth assays, MatTek dishes were coated (24 hr at 37°C) with 10% Matrigel mixed with either human IgG-Fc (Jackson Immunoresearch) or EphA4-Fc (R&D Systems). To precluster the Fc fusion proteins for some experiments, we combined each Fc protein with mouse anti-human Fc (Jackson Immunoresearch) for 1 hr at a 1:10 molar ratio. For each experiment, the spiral ganglion was removed at E12.5 and placed onto a precoated dish with normal culture medium and permitted to grow for 24 hr.

For neuron and mesenchyme coculture experiments, a spiral ganglion and an equivalent-sized portion of otic mesenchyme were removed from the cochlea at E12.5 and transferred to Matrigel-coated MatTek dishes (5% for 1 hr at 37°C), containing solutions of either standard control MO or a *Pou3f4*-specific MO (GATCCTCTACTAGTTATAATGTGGC). Neuron and mesenchyme explants were plated approximately 1 mm from each other before receiving Endo-Porter (0.6% final; Gene Tools) to facilitate delivery of the MOs. After 2 days at 37°C, the MO and Endo-Porter-containing medium was replaced with normal culture medium and grown an additional 3 days. For some experiments, soluble preclustered human IgG-Fc or EphA4-Fc was added to cultures following 2 days Morpholino exposure. Both IgG-Fc and EphA4-Fc were used at 10 nM based on a previous report (Brors et al., 2003). For culture experiments comparing Fc versus ephrin-B2-Fc (R&D Systems), we did not perform preclustering.

Chromatin Immunoprecipitation

ChIP was performed as described previously (Jhingory et al., 2010) but with minor modification. E15.5 cochleae were isolated in chilled PBS and then fixed for 20 min using 4% paraformaldehyde. The Agarose ChIP Kit (Pierce) was used for subsequent DNA digestion and precipitation. Approximately 8 µg of chicken anti-*Pou3f4* or chicken IgY (negative control) and PrecipHen beads (Aves Labs) was used for IP. With resulting DNAs, we performed qPCR using SYBR Green. For each primer set, a standard curve was generated using mouse genomic DNA; control and experimental C_t values were compared to this standard curve for quantification. The data here represent at least two independent ChIPs and three qPCR analyses for each primer set.

Please see *Supplemental Experimental Procedures* for lists of the antibodies, *in situ* hybridization probes, qPCR primers, quantification methods used in the study, and a description of the microarray that identified *Epha4*.

SUPPLEMENTAL INFORMATION

Supplemental Information includes four figures and Supplemental Experimental Procedures and can be found with this article online at doi:10.1016/j.neuron.2011.10.029.

ACKNOWLEDGMENTS

We thank the members of the Kelley laboratory for their valuable discussions and technical assistance during this work. We thank Dr. Lisa Cunningham (NIH/National Institute on Deafness and other Communication Disorders [NIDCD]), Dr. Doris Wu (NIH/NIDCD), and Dr. Maria J. Donoghue (Georgetown University) for the critical reading of this manuscript. *Epha4* null tissue was a kind gift from Dr. Maria J. Donoghue. Mr. Jonathan Stuckey was very helpful

with the illustration in Figure 8. The National Deafness and Other Communication Disorders Intramural Research Program funded this work.

Accepted: October 5, 2011

Published: January 11, 2012

REFERENCES

- Ahn, K.J., Passero, F., Jr., and Crenshaw, E.B., 3rd. (2009). Otic mesenchyme expression of Cre recombinase directed by the inner ear enhancer of the Brn4/Pou3f4 gene. *Genesis* 47, 137–141.
- Appler, J.M., and Goodrich, L.V. (2011). Connecting the ear to the brain: Molecular mechanisms of auditory circuit assembly. *Prog. Neurobiol.* 93, 488–508.
- Baum, P.D., and Garriga, G. (1997). Neuronal migrations and axon fasciculation are disrupted in ina-1 integrin mutants. *Neuron* 19, 51–62.
- Bianchi, L.M., and Gale, N.W. (1998). Distribution of Eph-related molecules in the developing and mature cochlea. *Hear. Res.* 117, 161–172.
- Bossing, T., and Brand, A.H. (2002). Dephrrin, a transmembrane ephrin with a unique structure, prevents interneuronal axons from exiting the Drosophila embryonic CNS. *Development* 129, 4205–4218.
- Breuskin, I., Bodson, M., Thelen, N., Thiry, M., Borgs, L., Nguyen, L., Stolt, C., Wegner, M., Lefebvre, P.P., and Malgrange, B. (2010). Glial but not neuronal development in the cochleo-vestibular ganglion requires Sox10. *J. Neurochem.* 114, 1827–1839.
- Brors, D., Bodmer, D., Pak, K., Aletsee, C., Schäfers, M., Dazert, S., and Ryan, A.F. (2003). EphA4 provides repulsive signals to developing cochlear ganglion neurites mediated through ephrin-B2 and -B3. *J. Comp. Neurol.* 462, 90–100.
- Carney, P.R., and Silver, J. (1983). Studies on cell migration and axon guidance in the developing distal auditory system of the mouse. *J. Comp. Neurol.* 215, 359–369.
- Coate, T.M., Swanson, T.L., and Copenhaver, P.F. (2009). Reverse signaling by glycosylphosphatidylinositol-linked Manduca ephrin requires a SRC family kinase to restrict neuronal migration in vivo. *J. Neurosci.* 29, 3404–3418.
- Cowan, C.A., and Henkemeyer, M. (2001). The SH2/SH3 adaptor Grb4 transduces B-ephrin reverse signals. *Nature* 413, 174–179.
- Davis, S., Gale, N.W., Aldrich, T.H., Maisonnier, P.C., Lhotak, V., Pawson, T., Goldfarb, M., and Yancopoulos, G.D. (1994). Ligands for EPH-related receptor tyrosine kinases that require membrane attachment or clustering for activity. *Science* 266, 816–819.
- Driver, E.C., and Kelley, M.W. (2009). Specification of cell fate in the mammalian cochlea. *Birth Defects Res. C Embryo Today* 87, 212–221.
- Driver, E.C., Pryor, S.P., Hill, P., Turner, J., Rüther, U., Biesecker, L.G., Griffith, A.J., and Kelley, M.W. (2008). Hedgehog signaling regulates sensory cell formation and auditory function in mice and humans. *J. Neurosci.* 28, 7350–7358.
- Eberhart, J., Swartz, M.E., Koblar, S.A., Pasquale, E.B., and Krull, C.E. (2002). EphA4 constitutes a population-specific guidance cue for motor neurons. *Dev. Biol.* 247, 89–101.
- Fekete, D.M., and Campero, A.M. (2007). Axon guidance in the inner ear. *Int. J. Dev. Biol.* 51, 549–556.
- Fritzsch, B., Pauley, S., Matei, V., Katz, D.M., Xiang, M., and Tessarollo, L. (2005). Mutant mice reveal the molecular and cellular basis for specific sensory connections to inner ear epithelia and primary nuclei of the brain. *Hear. Res.* 206, 52–63.
- Gallarda, B.W., Bonanomi, D., Müller, D., Brown, A., Alaynick, W.A., Andrews, S.E., Lemke, G., Pfaff, S.L., and Marquardt, T. (2008). Segregation of axial motor and sensory pathways via heterotypic trans-axonal signaling. *Science* 320, 233–236.
- Gerety, S.S., and Anderson, D.J. (2002). Cardiovascular ephrinB2 function is essential for embryonic angiogenesis. *Development* 129, 1397–1410.
- Helmbacher, F., Schneider-Maunoury, S., Topilko, P., Tiret, L., and Charnay, P. (2000). Targeting of the EphA4 tyrosine kinase receptor affects dorsal/ventral pathfinding of limb motor axons. *Development* 127, 3313–3324.
- Hsieh, C.Y., Hong, C.T., and Cramer, K.S. (2007). Deletion of EphA4 enhances deafferentation-induced ipsilateral sprouting in auditory brainstem projections. *J. Comp. Neurol.* 504, 508–518.
- Huai, J., and Drescher, U. (2001). An ephrin-A-dependent signaling pathway controls integrin function and is linked to the tyrosine phosphorylation of a 120-kDa protein. *J. Biol. Chem.* 276, 6689–6694.
- Huang, L.C., Thorne, P.R., Housley, G.D., and Montgomery, J.M. (2007). Spatiotemporal definition of neurite outgrowth, refinement and retraction in the developing mouse cochlea. *Development* 134, 2925–2933.
- Huffman, K.J., and Cramer, K.S. (2007). EphA4 misexpression alters tonotopic projections in the auditory brainstem. *Dev. Neurobiol.* 67, 1655–1668.
- Jhingory, S., Wu, C.Y., and Taneyhill, L.A. (2010). Novel insight into the function and regulation of alphaN-catenin by Snail2 during chick neural crest cell migration. *Dev. Biol.* 344, 896–910.
- Kandpal, G., Jacob, A.N., and Kandpal, R.P. (1996). Transcribed sequences encoded in the region involved in contiguous deletion syndrome that comprises X-linked stapes fixation and deafness. *Somat. Cell Mol. Genet.* 22, 511–517.
- Kelley, M.W. (2006). Regulation of cell fate in the sensory epithelia of the inner ear. *Nat. Rev. Neurosci.* 7, 837–849.
- Koundakjian, E.J., Appler, J.L., and Goodrich, L.V. (2007). Auditory neurons make stereotyped wiring decisions before maturation of their targets. *J. Neurosci.* 27, 14078–14088.
- Kullander, K., and Klein, R. (2002). Mechanisms and functions of Eph and ephrin signalling. *Nat. Rev. Mol. Cell Biol.* 3, 475–486.
- Lin, D.M., Fetter, R.D., Kopczynski, C., Grenningloh, G., and Goodman, C.S. (1994). Genetic analysis of Fasciclin II in Drosophila: defasciculation, refasciculation, and altered fasciculation. *Neuron* 13, 1055–1069.
- Meier, S., Sprecher, S.G., Reichert, H., and Hirth, F. (2006). Ventral veins lacking is required for specification of the tritocerebrum in embryonic brain development of Drosophila. *Mech. Dev.* 123, 76–83.
- Mellitzer, G., Xu, Q., and Wilkinson, D.G. (1999). Eph receptors and ephrins restrict cell intermingling and communication. *Nature* 400, 77–81.
- Meyer, A.C., Frank, T., Khimich, D., Hoch, G., Riedel, D., Chapochnikov, N.M., Yarin, Y.M., Harke, B., Hell, S.W., Egner, A., and Moser, T. (2009). Tuning of synapse number, structure and function in the cochlea. *Nat. Neurosci.* 12, 444–453.
- Miko, I.J., Henkemeyer, M., and Cramer, K.S. (2008). Auditory brainstem responses are impaired in EphA4 and ephrin-B2 deficient mice. *Hear. Res.* 235, 39–46.
- Minowa, O., Ikeda, K., Sugitani, Y., Oshima, T., Nakai, S., Katori, Y., Suzuki, M., Furukawa, M., Kawase, T., Zheng, Y., et al. (1999). Altered cochlear fibrocytes in a mouse model of DFNB3 nonsyndromic deafness. *Science* 285, 1408–1411.
- Montcouquiol, M., Rachel, R.A., Lanford, P.J., Copeland, N.G., Jenkins, N.A., and Kelley, M.W. (2003). Identification of Vangl2 and Scrb1 as planar polarity genes in mammals. *Nature* 423, 173–177.
- Mukai, S., Nakagawa, H., Ichikawa, H., Miyazaki, S., Nishimura, K., and Matsuo, S. (2011). Effects of extracellular acidic-alkaline stresses on trigeminal ganglion neurons in the mouse embryo in vivo. *Arch. Toxicol.* 85, 149–154.
- Nemzou, N.R.M., Bulankina, A.V., Khimich, D., Giese, A., and Moser, T. (2006). Synaptic organization in cochlear inner hair cells deficient for the CaV1.3 (alpha1D) subunit of L-type Ca²⁺ channels. *Neuroscience* 141, 1849–1860.
- North, H.A., Zhao, X., Kolk, S.M., Clifford, M.A., Ziskind, D.M., and Donoghue, M.J. (2009). Promotion of proliferation in the developing cerebral cortex by EphA4 forward signaling. *Development* 136, 2467–2476.
- Okazawa, H., Imafuku, I., Minowa, M.T., Kanazawa, I., Hamada, H., and Mouradian, M.M. (1996). Regulation of striatal D1A dopamine receptor gene transcription by Brn-4. *Proc. Natl. Acad. Sci. USA* 93, 11933–11938.

- Orioli, D., Henkemeyer, M., Lemke, G., Klein, R., and Pawson, T. (1996). Sek4 and Nuk receptors cooperate in guidance of commissural axons and in palate formation. *EMBO J.* 15, 6035–6049.
- Pan, L., Deng, M., Xie, X., and Gan, L. (2008). ISL1 and BRN3B co-regulate the differentiation of murine retinal ganglion cells. *Development* 135, 1981–1990.
- Pasquale, E.B. (2005). Eph receptor signalling casts a wide net on cell behaviour. *Nat. Rev. Mol. Cell Biol.* 6, 462–475.
- Phillips, K., and Luisi, B. (2000). The virtuoso of versatility: POU proteins that flex to fit. *J. Mol. Biol.* 302, 1023–1039.
- Phippard, D., Heydemann, A., Lechner, M., Lu, L., Lee, D., Kyin, T., and Crenshaw, E.B., 3rd. (1998). Changes in the subcellular localization of the Brn4 gene product precede mesenchymal remodeling of the otic capsule. *Hear. Res.* 120, 77–85.
- Phippard, D., Lu, L., Lee, D., Saunders, J.C., and Crenshaw, E.B., 3rd. (1999). Targeted mutagenesis of the POU-domain gene Brn4/Pou3f4 causes developmental defects in the inner ear. *J. Neurosci.* 19, 5980–5989.
- Pickles, J.O., Claxton, C., and Van Heumen, W.R. (2002). Complementary and layered expression of Ephs and ephrins in developing mouse inner ear. *J. Comp. Neurol.* 449, 207–216.
- Puligilla, C., and Kelley, M.W. (2009). Building the world's best hearing aid: regulation of cell fate in the cochlea. *Curr. Opin. Genet. Dev.* 19, 368–373.
- Puligilla, C., Dabdoub, A., Brenowitz, S.D., and Kelley, M.W. (2010). Sox2 induces neuronal formation in the developing mammalian cochlea. *J. Neurosci.* 30, 714–722.
- Raft, S., Koundakjian, E.J., Quinones, H., Jayasena, C.S., Goodrich, L.V., Johnson, J.E., Segil, N., and Groves, A.K. (2007). Cross-regulation of Ngn1 and Math1 coordinates the production of neurons and sensory hair cells during inner ear development. *Development* 134, 4405–4415.
- Rubel, E.W., and Fritzsch, B. (2002). Auditory system development: primary auditory neurons and their targets. *Annu. Rev. Neurosci.* 25, 51–101.
- Ruben, R.J. (1967). Development of the inner ear of the mouse: a radioautographic study of terminal mitoses. *Acta Otolaryngol. Suppl.* 220, 221–244.
- Ryan, A.K., and Rosenfeld, M.G. (1997). POU domain family values: flexibility, partnerships, and developmental codes. *Genes Dev.* 11, 1207–1225.
- Samadi, D.S., Saunders, J.C., and Crenshaw, E.B., 3rd. (2005). Mutation of the POU-domain gene Brn4/Pou3f4 affects middle-ear sound conduction in the mouse. *Hear. Res.* 199, 11–21.
- Simmons, D., Duncan, J., Caprona, D.C., and Fritzsch, B. (2011). Development of the inner ear efferent system. In *Auditory and Vestibular Efferents*, D.K. Ryugo, R.R. Fay, and A.N. Popper, eds. (New York: Springer).
- Smith, C.A. (1961). Innervation pattern of the cochlea. The internal hair cell. *Trans. Am. Otol. Soc.* 49, 35–60.
- Tessier-Lavigne, M., and Goodman, C.S. (1996). The molecular biology of axon guidance. *Science* 274, 1123–1133.
- van Heumen, W.R., Claxton, C., and Pickles, J.O. (2000). Expression of EphA4 in developing inner ears of the mouse and guinea pig. *Hear. Res.* 139, 42–50.
- Wang, L., Klein, R., Zheng, B., and Marquardt, T. (2011). Anatomical coupling of sensory and motor nerve trajectory via axon tracking. *Neuron* 71, 263–277.
- Wilkinson, D.G. (2001). Multiple roles of EPH receptors and ephrins in neural development. *Nat. Rev. Neurosci.* 2, 155–164.
- Zhou, C.Q., Lee, J., Henkemeyer, M.J., and Lee, K.H. (2011). Disruption of ephrin B/Eph B interaction results in abnormal cochlear innervation patterns. *Laryngoscope* 121, 1541–1547.